Journal of Photochemistry & Photobiology, B: Biology 159 (2016) 196–204

Contents lists available at ScienceDirect

Journal of Photochemistry & Photobiology, B: Biology

journal homepage: www.elsevier.com/locate/jphotobiol

Silicon(IV) phthalocyanines substituted axially with different nucleoside moieties. Effects of nucleoside type on the photosensitizing efficiencies and *in vitro* photodynamic activities

Bi-Yuan Zheng, Xiao-Min Shen, Dong-Mei Zhao, Yi-Bin Cai, Mei-Rong Ke, Jian-Dong Huang

College of Chemistry, State Key Laboratory of Photocatalysis on Energy and Environment, Fuzhou University, Fuzhou 350108, China

ARTICLE INFO

Article history:
Received 10 August 2015
Received in revised form 28 March 2016
Accepted 29 March 2016
Available online 08 April 2016

Keywords:
Silicon(IV) phthalocyanine
Photosensitizer
Photodynamic therapy
Nucleoside
Singlet oxygen quantum yields

ABSTRACT

A series of new silicon(IV) phthalocyanines (SiPcs) di-substituted axially with different nucleoside moieties have been synthesized and evaluated for their singlet oxygen quantum yields (Φ_Δ) and *in vitro* photodynamic activities. The adenosine-substituted SiPc shows a lower photosensitizing efficiency ($\Phi_\Delta = 0.35$) than the uridine- and cytidine-substituted analogs ($\Phi_\Delta = 0.42$–0.44), while the guanosine-substituted SiPc exhibits a weakest singlet oxygen generation efficiency with a Φ_Δ value down to 0.03. On the other hand, replacing axial adenosines with chloro-modified adenosines and purines can result in the increase of photogenerating singlet oxygen efficiencies of SiPcs. The formed SiPcs **1** and **2**, which contain monochloro-modified adenosines and dichloro-modified purines respectively, appear as efficient photosensitizers with Φ_Δ of 0.42–0.44. Both compounds **1** and **2** present high photocytotoxicities against HepG2 and BGC823 cancer cells with IC_{50} values ranging from 9 nM to 33 nM. The photocytotoxicities of these two compounds are remarkably higher than the well-known anticancer photosensitizer, chlorin e6 ($IC_{50} = 752$ nM against HepG2 cells) in the same condition. As revealed by confocal microscopy, for both cell lines, compound **1** can essentially bind to mitochondria, while compound **2** is just partially localized in mitochondria. In addition, the two compounds induce cell death of HepG2 cells likely through apoptosis.

1. Introduction

Photodynamic therapy (PDT) has attracted considerable attention as a promising minimal-invasive treatment for both neoplastic and non-neoplastic diseases [1–4]. One of the prominent advantages of PDT lies in its ability to eradicate malignant tissue without systemic toxicity, which is a major drawback of traditional therapeutic methods like chemotherapy and radiotherapy. PDT typically involves the systemic administration of a photosensitizer and the tumor-oriented illumination with a light of specific wavelength to generate reactive oxygen species (ROS), particularly singlet oxygen, leading to cell and tissue damage. The overall efficacy of the treatment depends greatly on the behavior of photosensitizers. As a result, various strategies have been developed to obtain a favorable photosensitizer [4–11]. Among these approaches, the conjugation of a photosensitizer with biological ligands (such as antibodies, peptides, carbohydrates, and folic acid), which are capable of improving the biocompatibility and tumor-targeting of the photosensitizers, has received a great deal of interest [6–13].

Having a number of advantageous characteristics, such as intense absorption in the "phototherapeutic window" (650–800 nm), low dark toxicity, and ease of chemical modification, phthalocyanines have been found to be highly promising as second-generation photosensitizers for PDT [2–4,12–16]. The introduction of biomolecules on the axial positions of phthalocyanines has appeared as an efficient and promising approach to obtain the desirable phthalocyanine-based photosensitizers [17–22]. Apart from aforementioned improvement of biocompatibility and tumor-targeting, the method could effectively decrease intrinsic aggregated propensity of phthalocyanines, which will lead to inefficient ROS generation and poor solubility in aqueous media. Among these biomolecules, we are particularly interested in nucleosides, which are important building blocks of DNA and RNA. Moreover, a number of nucleoside derivatives have been used as antiviral [23,24] and anticancer [25] drugs. However, the photobiological properties of phthalocyanines functionalized with nucleoside moieties remain hardly explored, although the synthesis and characterization of a few phthalocyanine-nucleoside conjugates have been reported [18,26–31].

Very recently, our group have reported the photodynamic activities of a series of silicon(IV) phthalocyanines (SiPcs) axially disubstituted with uridine and cytidine moieties in a preliminary communication [18]. As an extension of this study, we report herein four new analogs axially disubstituted with adenosine, purine, and guanosine derivatives, including their synthesis, spectroscopic properties, singlet oxygen generation efficiencies, and *in vitro* photodynamic activities against

E-mail address: jdhuang@fzu.edu.cn (J.-D. Huang).

http://dx.doi.org/10.1016/j.jphotobiol.2016.03.055
1011-1344/

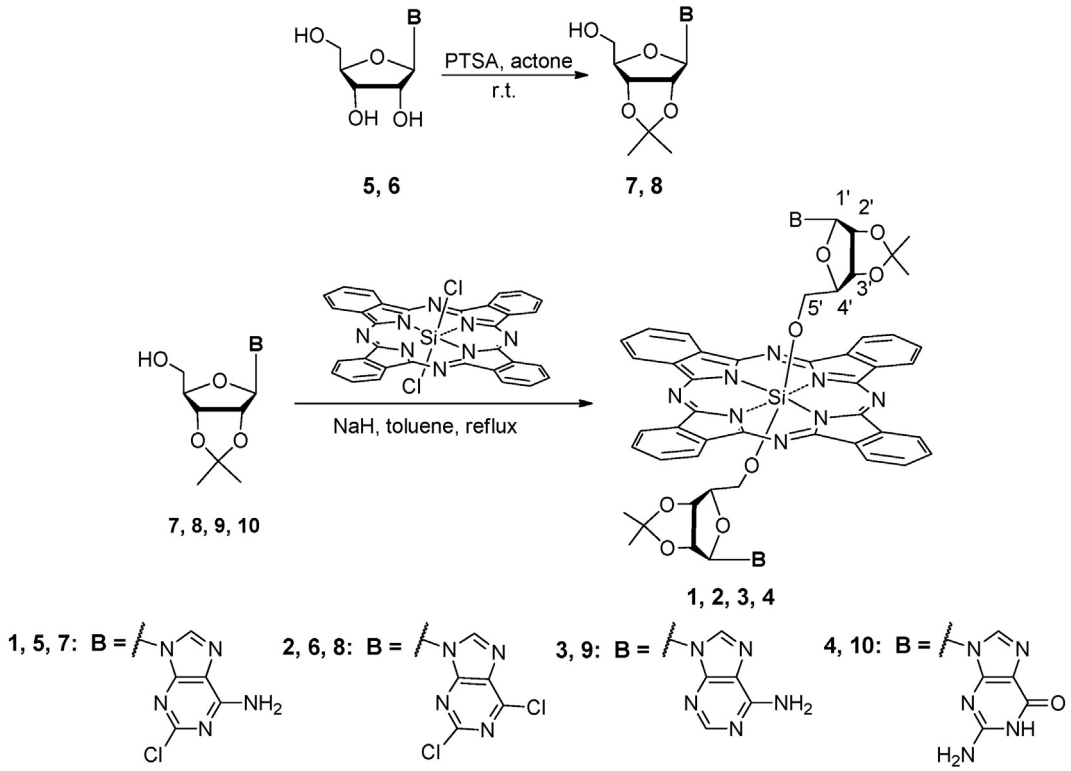

Scheme 1. Preparation of SiPcs **1–4**.

HepG2 and BGC823 cells. With the goal of understanding the structure–activity relationship of this intriguing class of novel nucleoside-containing photosensitizer, the effects of nucleoside type on the photochemical properties and *in vitro* photodynamic activities have been discussed.

2. Experimental Section

2.1. General

All the reactions were performed under an atmosphere of nitrogen. Acetone and toluene were distilled from anhydrous calcium sulfate and sodium, respectively. 2′,3′-o-isopropyl-adenosin (**9**) and 2′,3′-o-isopropyl-guanosine (**10**) were purchased from Acros. Cremophor EL and ZnPc were obtained from Sigma Aldrich. Ce6 was obtained from J&K Scientific. Chromatographic purifications were performed on silica gel columns (100–200 mesh, Qingdao Haiyang Chemical Co., Ltd., China) with the indicated eluents. Size exclusion chromatography was performed on Bio-Rad Bio-Beads S-X3 beads with the indicated eluents. All other solvents and reagents were of reagent grade and used as received.

Table 1
Photophysical and photochemical data for SiPcs **1–4** and **11–12** in DMF.

SiPcs	λ_{max} (nm)	λ_{em} (nm)a	Stokes shift (nm)	$\varepsilon \times 10^5$ ($M^{-1}\cdot cm^{-1}$)	Φ_Fb	Φ_Δc
1	677	685	8	1.77	0.34	0.42
2	679	687	8	1.92	0.25	0.44
3	677	686	9	1.80	0.30	0.35
4	676	682	6	1.80	0.02	0.03
11 [18]	678	687	9	2.00	0.37	0.44
12 [18]	677	685	8	2.13	0.36	0.42

[a] Excited at 610 nm.
[b] Using ZnPc in DMF as the reference ($\Phi_F = 0.28$) [33].
[c] Determined by using DPBF as chemical quencher, and ZnPc in DMF as the reference ($\Phi_\Delta = 0.56$) [34].

1H NMR spectra were recorded on Bruker a AVANCE III 400 or 500 spectrometer in DMSO-d6 and $CDCl_3$. Chemical shifts were relative to internal $SiMe_4$ ($\delta = 0$ ppm). High resolution mass spectra were recorded on an Agilent ESI-Q-Tof 6520 mass spectrometer or a Thermo Fisher Scientific Exactive Plus Orbitrap LC–MS spectrometer. Electronic absorption spectra were measured on a Shimadzu UV-2450 UV–vis spectrophotometer. Fluorescence spectra were taken on an Edinburgh FL900/FS900 spectrofluorometer. Φ_F and Φ_Δ were determined as described in our previous manuscripts [18,32].

The purity of all the new phthalocyanines was determined by HPLC and was found to be ≥95%. The analytical HPLC experiments were performed on a Kromasir KR100-10C18 column (5 μm, 4.6 mm × 250 mm) by using a Shimadzu LC-10AT controller with a SPD-M10A diode array detector. The conditions were set as follows: mobile phase from 5% B changed to 95% B over 30 min, then maintained 95% B for a further 20 min (solvent A = distilled water; solvent B = DMF). The column temperature was set at 30 °C. The flow-rate was fixed at 0.5 ml min^{-1}.

Statistical analyses were performed by using the Student's *t*-test. *P* values of 0.05 were considered as statistically significant.

2.2. Synthesis

2′,3′-o-isopropyl-2-chloro-adenosin (7). A mixture of *p*-toluenesulfonic acid (PTSA) (1.72 g, 10 mmol) and dry acetone (20 ml) was added dropwise into a stirring mixture of 2-chloro-adenosin (309 mg, 1 mmol) and dry acetone (20 ml) in ice-water bath. The mixture was stirred at room temperature for 22 h and then was poured into ice sodium bicarbonate solution (4% w.t.) with stirring until the bubble disappeared. The liquid was then extracted with CH_2Cl_2 for three times. The organic layers were dried over anhydrous $MgSO_4$ and concentrated to afford a faint yellow solid **7** (283 mg, 83%). 1H NMR (400 MHz, DMSO-d6): δ = 8.37 (s, 1H, imidazole-H), 7.89 (br., 2H, NH_2), 6.06 (d, J = 2.4 Hz, 1H, 1′-H), 5.28–5.30 (m, 1H, 2′-H), 5.10–5.12 (m, 1H, OH), 4.93–4.95 (m, 1H, 3′-H), 4.21–4.23 (m, 1H, 4′-H), 3.54–3.57 (m, 2H, 5′-H), 1.55 (s, 3H, CH_3), 1.33 ppm (s, 3H, CH_3);

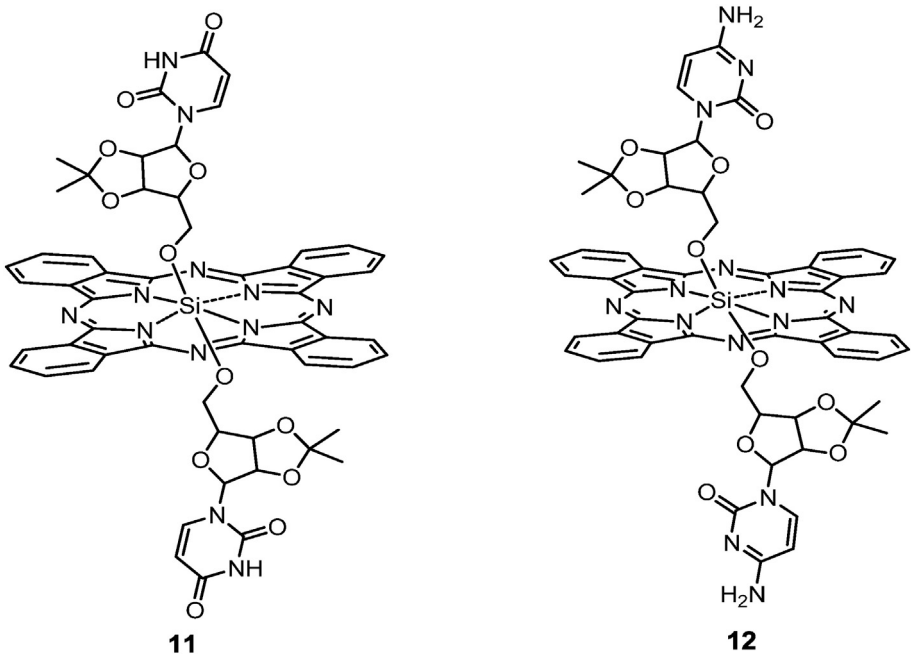

Fig. 1. Structures of silicon(IV) phthalocyanines **11** and **12**.

HRMS (ESI) *m/z* $[M + H]^+$ calcd. for $C_{13}H_{17}ClN_5O_4$: 342.0969, found: 342.0968.

2′,3′-o-isopropyl-2,6-dichloropurine riboside (8). According to the above procedure, a solution of 2,6-dichloropurine riboside (321 mg, 1 mmol) in dry acetone (20 ml) was treated with PTSA (1.72 g, 10 mmol) in dry acetone (20 ml) for 16 h and neutralized with ice sodium bicarbonate solution (4 wt.%) to afford a clear solution, which was extracted with CH_2Cl_2 for three times. The organic layers were dried over anhydrous $MgSO_4$ and concentrated to afford crude product, which was further purified by column chromatography (silica gel) with ethyl acetate as eluent. The main component was collected and concentrated to give a white solid **8** (324 mg, 90%). 1H NMR (500 MHz, $CDCl_3$): δ = 8.33 (s, 1H, imidazole-H), 6.01 (d, J = 4.5 Hz, 1H, 1′-H), 5.17–5.19 (m, 1H, 2′-H), 5.11–5.13 (m, 1H, 3′-H), 4.54–4.55 (m, 1H, 4′-H), 4.31 (br., 1H, OH), 4.00–4.02 (m, 1H, 5′-H), 3.85–3.88 (m, 1H, 5′-H), 1.66 (s, 3H, CH_3), 1.40 (s, 3H, CH_3), 1.26 ppm (s, 3H, CH_3); HRMS (ESI) *m/z* $[M + Cl]^-$ calcd. for $C_{13}H_{14}Cl_3N_4O_4$: 395.0081, found: 395.0094.

Silicon phthalocyanine 1. A mixture of $SiPcCl_2$ (40 mg, 0.065 mmol), adenosin **7** (177 mg, 0.52 mmol), and NaH (0.42 mmol) were refluxed in toluene (20 ml) for 24 h. After evaporating the solvent *in vacuo*, the residue was dissolved in CH_2Cl_2 and then washed with water. The organic layers were collected, dried over anhydrous $MgSO_4$, and concentrated to afford crude product, which was further purified by column chromatography (silica gel) using tetrahydrofuran (THF) as eluent, followed by size-exclusion chromatography by using THF as the eluent to give a blue solid **1** (48 mg, 60%). UV–vis (DMF): λ_{max}, nm (ε, $M^{-1}\cdot cm^{-1}$) 677 (177,000). 1H NMR (500 MHz, $CDCl_3$): δ = 9.62–9.63 (m, 8H, Pc-H_α), 8.39–8.41 (m, 8H, Pc-H_β), 6.43 (s, 4H, NH_2), 5.39 (s, 2H, imidazole-H), 4.58 (d, J = 3.0 Hz, 2H, 1′-H), 2.18–2.19 (m, 2H, 2′-H), 1.80 (s, 2H, 3′-H), 0.92 (s, 6H, CH_3), 0.89–0.91 (m, 2H, 4′-H), 0.76 (s, 6H, CH_3), −1.28 (dd, J = 12.0, 2.5 Hz, 2H, 5′-H), −2.29 ppm (dd, J = 12.0, 3.5 Hz, 2H, 5′-H); HRMS (ESI) *m/z* $[M + Na]^+$ calcd. for $C_{58}H_{46}Cl_2N_{18}NaO_8Si$: 1243.2790; found: 1243.2788.

Silicon phthalocyanine 2. According to the procedure described for SiPc **1**, $SiPcCl_2$ (40 mg, 0.065 mmol) was treated with dichloropurine riboside **8** (187 mg, 0.52 mmol), and NaH (0.42 mmol) in toluene (20 ml) to give **2** as a blue solid (53 mg, 65%). UV–vis (DMF): λ_{max}, nm (ε, $M^{-1}\cdot cm^{-1}$) 679 (192,000). 1H NMR (500 MHz, $CDCl_3$): δ = 9.56–9.58 (m, 8H, Pc-H_α), 8.44–8.46 (m, 8H, Pc-H_β), 5.45 (s, 2H, imidazole-H), 4.50 (d, J = 2.5 Hz, 2H, 1′-H), 1.98 (s, 2H, 2′-H), 1.92–

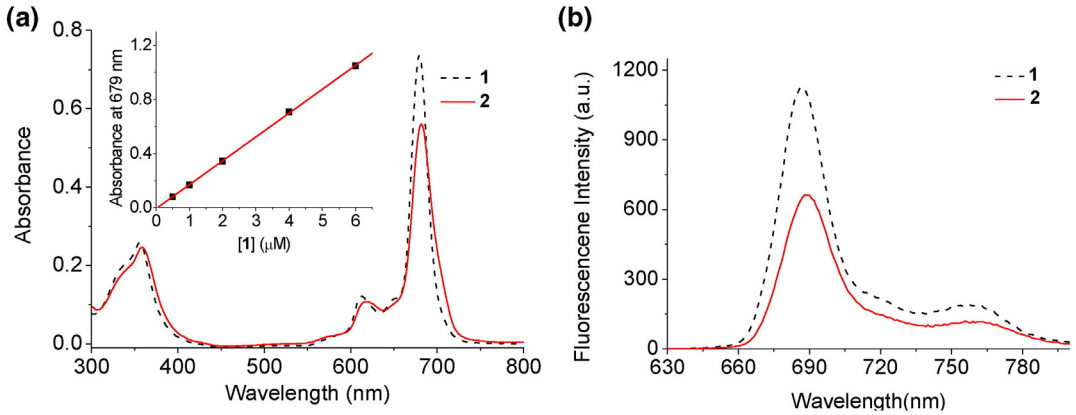

Fig. 2. (a) UV–vis absorption spectra of SiPcs **1** and **2** (4 μM), formulated with 0.05% Cremophor EL, in RPMI 1640 cellular culture medium. The inset plots the Q-band absorbance *versus* the concentration of **1**. (b) Fluorescence spectra of SiPcs **1** and **2** in RPMI 1640 cellular culture medium (formulated with 0.05% Cremophor EL) (both at 4 μM, λex = 610 nm). (For interpretation of the references to color in this figure, the reader is referred to the web version of this article.)

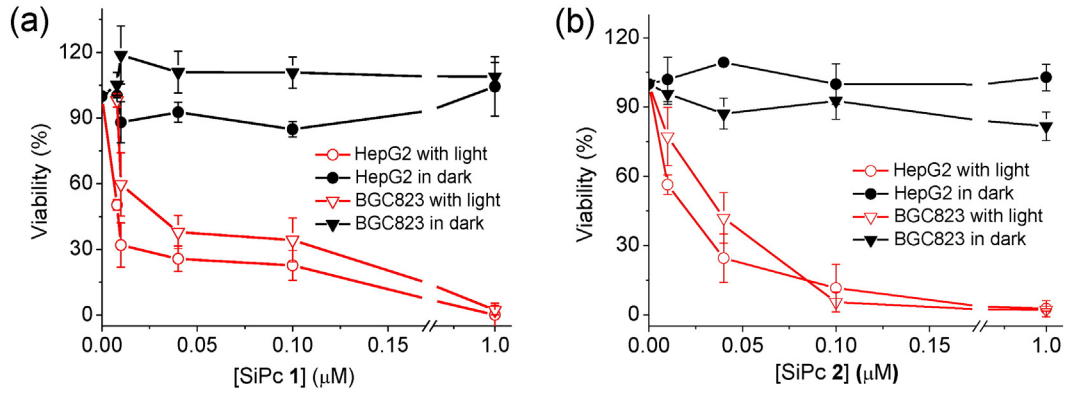

Fig. 3. Comparison of the cytotoxic effects of SiPcs (a) **1** and (b) **2** on HepG2 and BGC823 cells in the absence and presence of light (λ > 610 nm) at a dose of 27 J·cm^{-2}. Values represent mean ± standard deviation of three separate experiments.

1.94 (m, 2H, 3′-H), 0.94 (s, 6H, CH_3), 0.85 (s, 6H, CH_3), 0.73–0.74 (m, 2H, 4′-H), −1.19 (dd, J = 12.0, 2.0 Hz, 2H, 5′-H), −2.45 ppm (dd, J = 12.0, 3.0 Hz, 2H, 5′-H); HRMS (ESI) m/z $[M]^-$ calcd. for $C_{58}H_{42}Cl_4N_{16}O_8Si$: 1260.1865; found: 1260.1877.

Silicon phthalocyanine 3. According to the procedure described for SiPc **1**, $SiPcCl_2$ (40 mg, 0.065 mmol) was treated with adenosin **9** (160 mg, 0.52 mmol), and NaH (0.42 mmol) in toluene (20 ml) to give **3** as a blue solid (42 mg, 56%). UV–vis (DMF): λ_{max}, nm (ε, $M^{-1}\cdot cm^{-1}$) 677 (180,000). 1H NMR (400 MHz, $CDCl_3$): δ = 9.55–9.57 (m, 8H, Pc-H_α), 8.36–8.38 (m, 8H, Pc-H_β), 8.02 (s, 2H, pyrimidine-H), 5.65 (s, 4H, NH_2), 5.37 (s, 2H, imidazole-H), 4.50 (d, J = 5.4 Hz, 2H, 1′-H), 2.13 (s, 2H, 2′-H), 0.91 (s, 6H, CH_3), 0.78 (s, 6H, CH_3), 0.69–0.71 (d, J = 6.0 Hz, 2H, 3′-H), 0.07 (s, 2H, 4′-H), −1.37–−1.35 (m, 2H, 5′-H), −2.37–−2.33 (m, 2H, 5′-H). HRMS (ESI) m/z $[M + Na]^+$ calcd. for $C_{58}H_{48}N_{18}$ NaO_8Si: 1175.3569; found: 1175.3550.

Silicon phthalocyanine 4. According to the procedure described for SiPc **1**, $SiPcCl_2$ (40 mg, 0.065 mmol) was treated with guanosine **10** (168 mg, 0.52 mmol), and NaH (0.42 mmol) in toluene (20 ml) to give **4** as a blue solid (10 mg, 13%). UV–vis (DMF): λ_{max}, nm (ε, $M^{-1}\cdot cm^{-1}$) 676 (180,000). 1H NMR (400 MHz, d_6-DMSO): δ = 10.42–10.43 (d, J = 4.0 Hz, 2H, imidazole-NH), 9.62–9.64 (m, 8H, Pc-H_α), 8.49–8.51 (m, 8H, Pc-H_β), 7.95–7.96 (d, J = 4.0 Hz, 2H, imidazole-NH), 5.73–6.12 (m, 4H, NH_2), 4.46–4.47 (d, J = 4.0 Hz, 2H, 1′-H), 2.89–2.90 (d, J = 4.0 Hz, 2H, 2′-H), 2.73–2.75 (d, J = 8.0 Hz, 2H, 3′-H), 1.32–1.35 (d, 2H, J = 8.0 Hz, 4′-H), 0.75 (s, 6H, CH_3), 0.62 (s, 6H, CH_3), −1.62–−1.58 (m, J = 4.0 Hz, 2H, 5′-H), −2.20–−2.16 (m, J = 4.0 Hz, 2H, 5′-H). HRMS (ESI) m/z $[M + 2H]^{2+}$ calcd. for $C_{58}H_{50}N_{18}O_{10}Si$: 593.1864; found: 593.1877.

2.3. In Vitro Studies

The HepG2 human hepatocarcinoma cells and BGC823 human gastric cancer cells (from ATCC) were maintained in RPMI 1640 medium (Hyclone) supplemented with 10% fetal bovine serum, penicillin (50 units/ml), and streptomycin (50 μg/ml) at 37 °C in a humidified 5% CO_2 atmosphere.

Stock solutions of the studied SiPcs and Ce6 (all at 1 mM) were prepared in DMF and stored at 4 °C in the dark. The solution was then diluted to 80 μM with an aqueous solution of Cremophor (1%, 1 g in 100 ml of water), and further diluted with the cellular culture medium to appropriate concentrations.

Table 2
Comparison of the IC_{50} values of SiPcs **1, 2** and Ce6 against HepG2 and BGC823 cells.

SiPcs	IC_{50} (nM)	
	HepG2	BGC823
1	9	23
2	14	33
Ce6	750	–

***In vitro* photocytotoxicity.** The photocytotoxicity assay is the same as the procedure described previously [18]. Briefly, About 2 × 10^4 cells per well were seeded in 96-well plate and incubated overnight for cell adherence and growth. The cells were then incubated with 100 μl of the above phthalocyanine solutions for 2 h under the same conditions. After that, the cells were rinsed with PBS and re-fed with 100 μl of the culture medium before irradiated with 27 J/cm^2 of a red light (λ > 610 nm, 15 mW/cm^2 for 30 min).

Cell viability was determined by the colorimetric 3-(4,5-dimethyl-2-thiazolyl) -2,5-diphenyl-2*H*-tetrazolium bromide (MTT) assay. After illumination, the cells were incubated at 37 °C under 5% CO_2 overnight. An MTT (Sigma) solution in PBS (20 μl, 5 mg/ml) was added to each well followed by incubation for 4 h under the same environment. A 200 μl of DMSO was then added to each well. The 96-well plate was agitated on a Thermo-Labsystems microplate reader (Multishan MK3) at ambient temperature for 20 s before the absorbance at 490 nm at each well was taken. The average absorbance of the blank wells, which did not contain the cells, was subtracted from the readings of the other wells. The cell viability was then determined by the equation: Cell Viability (%) = $[\Sigma(A_i / \bar{A}_{control} \times 100)] / n$, where A_i is the absorbance of the ith data (i = 1, 2, …, n), $\bar{A}_{control}$ is the average absorbance of the control wells, in which the phthalocyanine was absent, and n (≥3) is the number of the data points.

Intracellular fluorescence studies. About 6 × 10^4 HepG2 cells in RPMI 1640 culture medium (0.5 ml) were seeded on a confocal dish and incubated overnight at 37 °C under 5% CO_2. After removing the medium, the cells were incubated with SiPcs **1**, **2**, or Ce6 (all at 2 μM) in the dark for 2 h, followed by being rinsed with PBS and viewed with a LEICA TCS SPE confocal microscope. Upon being excited at 635 nm under the same light intensity, the fluorescence signals of photosensitizers were monitored at 645–750 nm. The images were then digitized and analyzed by using the LEICA TCS SPE ROI Fluorescence Statistics. The intracellular fluorescence intensities (a total of 20 cells for each sample) were also determined.

Cellular uptake. About 6 × 10^5 HepG2 cells in RPMI 1640 culture medium (0.5 ml) were seeded on a confocal dish and incubated overnight at 37 °C under 5% CO_2. After removing the medium, the cells were incubated with SiPcs **1**, **2**, or Ce6 (all at 2 μM) in the dark for 2 h, followed by being rinsed with PBS, and then harvested by trypsin (0.25%) treatment. The trypsin was then quenched with the medium (0.5 ml). The solution was transferred to centrifuge tubes (1.5 ml) and centrifuged at 1000 rpm for 3 min. The pellet was then washed with PBS (1 ml) and the suspension was centrifuged again. After removing the PBS, the cells were lyzed with DMF (1.2 ml). The mixture was sonicated for 5 min and then centrifuged again. The supernatants were transferred for UV/Vis spectroscopic measurements. The absorbance at

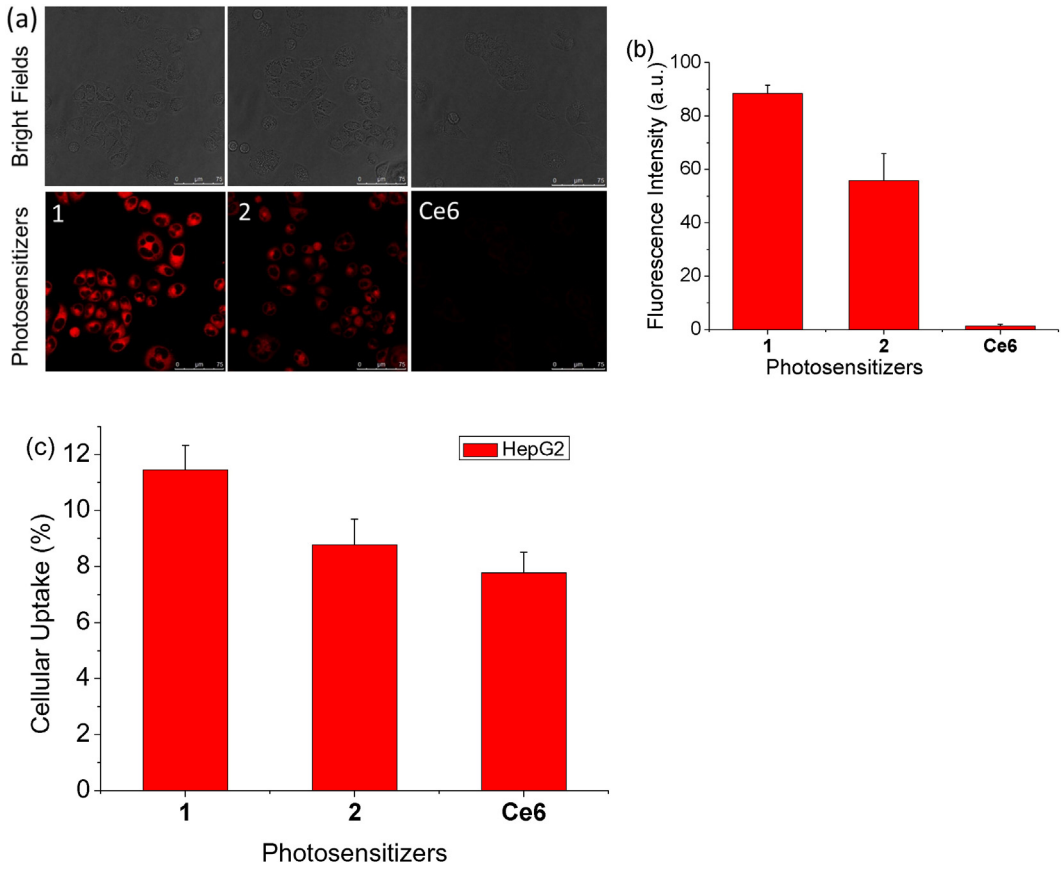

Fig. 4. (a) The bright field and intracellular fluorescence images of SiPcs **1**, **2**, and Ce6 (all at 2 μM) in HepG2 cells after incubation for 2 h. (b) Comparison of the corresponding intracellular fluorescence intensities of these photosensitizers. Data are expressed as the mean ± standard deviation (number of cells = 20). (c) Percentage cellular uptake for **1**, **2** and Ce6 determined by an extraction method. Data are expressed as mean value ± standard deviation of three independent experiments.

677 nm (**1**), 679 nm (**2**) or 663 nm (Ce6) was compared with the respective calibration curves to give the uptake concentrations.

Subcellular localization studies. About 6×10^4 HepG2 or BGC823 cells in the culture medium were seeded on a confocal dish. After removing the medium, the cells were incubated with the solutions of **1** or **2** in the medium (both at 2 μM, 0.5 ml) for 0.5 h under the same condition, and then Lyso Tracker Red (5 μM, 20 μl) was added for further 60 min co-incubation, followed by Mito Tracker Green (5 μM, 20 μl) for further 30 min co-incubation, leading to a total incubation time of 2 h for the photosensitizers, 1.5 h for Lyso Tracker Red, and 0.5 h for Mito Tracker Green. The cells were then rinsed with PBS and viewed with a LEICA TCS SPE confocal microscope equipped with 488 nm, 532 nm, and 635 nm solid-state lasers. MitoTracker Green and Lyso Tracker Red were excited at 488 nm and 532 nm monitored at 499–529 nm and 552–617 nm, respectively, while compounds **1** and **2** were excited at 635 nm and monitored at 645–750 nm. The subcellular localization of **1** and **2** were revealed by comparing the intracellular fluorescence images caused by MitoTracker Green, Lyso Tracker Red, and these phthalocyanines.

Apoptosis. About 1×10^5 HepG2 cells in the culture medium (0.5 ml) were seeded on a confocal dish (three dishes for each compound) and incubated overnight at 37 °C under 5% CO_2. After removing the medium, the cells were incubated with the solution of **1** or **2** in the medium (2 μM, 0.4 ml) for 2 h under the same conditions. The cells were then rinsed with PBS and refilled with 0.4 ml of the culture medium. Subsequently, two dishes of the cells were illuminated using a red light ($\lambda > 610$ nm, 15 mW/cm^2, 27 J/cm^2), and the third one was still kept in the dark for another 24 h as a control. After that, the illuminated cells were further incubated in the dark for 6 h and 24 h, respectively. At the set time, the cells were rinsed with PBS, followed by addition of 0.5 ml of binding buffer containing Annexin V-FITC (5 μl) and propidium iodium (PI) (5 μl), and further incubation at 37 °C for 10 min in the dark. The cells were then viewed using a LEICA TCS SPE fluorescence confocal microscope. Annexin V-FITC was excited at 488 nm and monitored at 499–529 nm, while PI was excited at 532 nm and monitored at 545–617 nm. The cell populations at different phase of cell death, namely viable (annexin V-FITC$^-$/PI$^-$), early apoptotic (annexin V-FITC$^+$/PI$^-$), and necrotic or late-stage apoptotic (annexin V-FITC$^+$/PI$^+$), were determined by digitally merging fluorescence images and phase contrast images.

3. Results and Discussion

3.1. Synthesis

Apart from the SiPcs axially di-substituted with isopropylidene-protected adenosines or guanosines (compounds **3** and **4**), we also prepared two analogs substituted with chloro-modified adenosines (**1**) and chloro-modified purines (**2**), on which one and two chlorine atom (s) have been introduced on the pyrimidine ring, respectively, in order to explore the effects of heavy atoms on the photosensitizing efficiency [20]. Scheme 1 shows the synthetic route of these SiPcs. Firstly, the isopropylidene-protected chloro-adenosine moieties **7** and dichloro-purine moieties **8** were prepared through a classical ketalation of the 2′,3′-hydroxyls of nucleoside derivatives **5** and **6** with acetone, respectively, using *p*-toluenesulfonic acid (PTSA) as a catalyst. On the other hand, the isopropylidene-protected adenosine **9** and guanosine **10** are commercially available. The compounds **7**–**10** were further treated with silicon(IV) phthalocyanine dichloride ($SiPcCl_2$), respectively, in the presence of NaH in toluene, leading to axial substitution, to give

the corresponding products **1–4**. The four final products are highly soluble in common organic solvents and could be readily purified by column chromatography.

3.2. Photophysical and Photochemical Properties

The spectroscopic properties of these compounds were measured in *N*,*N*-dimethylformamide (DMF), and the singlet oxygen quantum yields (Φ_Δ) of the four compounds **1–4** were also measured in DMF using 1,3-diphenylisobenzofuran (DPBF) as the scavenger [18]. The data are summarized in Table 1. For comparison, the data of analogs substituted with uridines and cytidines (compounds **10–11,** see Fig. 1) [18] are also added in Table 1.

The absorption spectra of the compounds **1–4** in DMF are similar with those of analogs **10–11**, showing an intense and sharp Q-band at 676–679 nm, as shown in Fig. S1. Their Q-bands strictly follow the Lambert–Beer law, indicating that these SiPcs are essentially free from aggregation in DMF. Upon excitation at 610 nm, the compounds **1–3** show a fluorescence emission at 685–687 nm with a fluorescence quantum yield (Φ_F) of 0.25–0.34 relative to unsubstituted zinc(II) phthalocyanine (ZnPc) ($\Phi_F = 0.28$) [33]. However, the guanosine-containing compound **4** exhibits an extremely weak fluorescence emission ($\Phi_F = 0.02$) (Table 1).

Moreover, the adenosine-substituted SiPc **3** presents a lower singlet oxygen generation efficiency ($\Phi_\Delta = 0.35$) than the uridine- and cytidine-substituted analogs **10–11** ($\Phi_\Delta = 0.42$–0.44), while the guanosine-substituted SiPc **4** exhibits a weakest photosensitizing efficiency with a Φ_Δ value down to 0.03. In other word, the introduction of adenosine and guanosine on the axial position of phthalocyanine resulted in the decrease of fluorescence and singlet oxygen quantum yields, when compared with introduction of uridine and cytidine. The reason for this observation is elusive at present, and we speculate that more nitrogen atoms on the bases of adenosine and guanosine probably results in relatively strong photoinduced electron transfer (PET) effect [21,35,36], thereby reducing the photosensitizing efficiency. For compound **4**, the primary amino group of the guanosine may be more close to the phthalocyanine ring spatially, producing a stronger quenching because of PET effect, and leading to the very weak fluorescence emission and singlet oxygen generation efficiencies.

On the other hand, replacing axial adenosines with chloro-modified adenosines can result in the increase of photogenerating singlet oxygen efficiencies of SiPcs. The formed SiPc **1** which contains monochloro-modified adenosines, appears as more efficient photosensitizers with Φ_Δ of 0.42, when compared with SiPc **3** containing adenosines. What is unexpected is its Φ_F value also increased from 0.30 to 0.34. This result could not be ascribed to heavy atom effect [20], but may be due to the electron-withdrawing effects of chlorine atom, which can decrease the PET effects of amine groups [36].

The electronic absorption spectra of **1** and **2** were further recorded in the Roswell Park Memorial Institute (RPMI) 1640 medium (formulated with 0.05% of Cremophor EL, wt.) to examine their aggregation behavior in a biological environment. As shown in Fig. 2a, the Q-bands of both compounds show slightly red-shift (2–3 nm) in the medium compared with that in DMF. For compound **1**, the Q-band (679 nm) remains very sharp and intense in the medium. As shown in the inset, the Q-band also strictly follows the Lambert–Beer law, suggesting compound **1** is essentially non-aggregated in the culture medium. But compound **2** presents relative broad Q-band (682 nm) with a slight decrease in intensity in contrast to compound **1**. It means that compound **2** shows a tiny tendency of aggregation in the aqueous condition. Their fluorescence spectra were also compared in RPMI medium. As shown in Fig. 2b, the fluorescence intensity of **2** in RPMI medium is obviously lower than **1**. The Φ_F values of **2** was calculated to be 0.17, which is also lower than that of **1** ($\Phi_F = 0.26$ for **1**). These observations suggest that compound **2** presented more aggregation trend than **1** in RPMI medium.

3.3. In Vitro Studies

3.3.1. Photocytotoxicities Against HepG2 and BGC823 Cells

In view of the higher singlet oxygen generation efficiency, the compounds **1** and **2** were chosen to evaluate their photodynamic activities against two different cell lines, namely, HepG2 human hepatocarcinoma

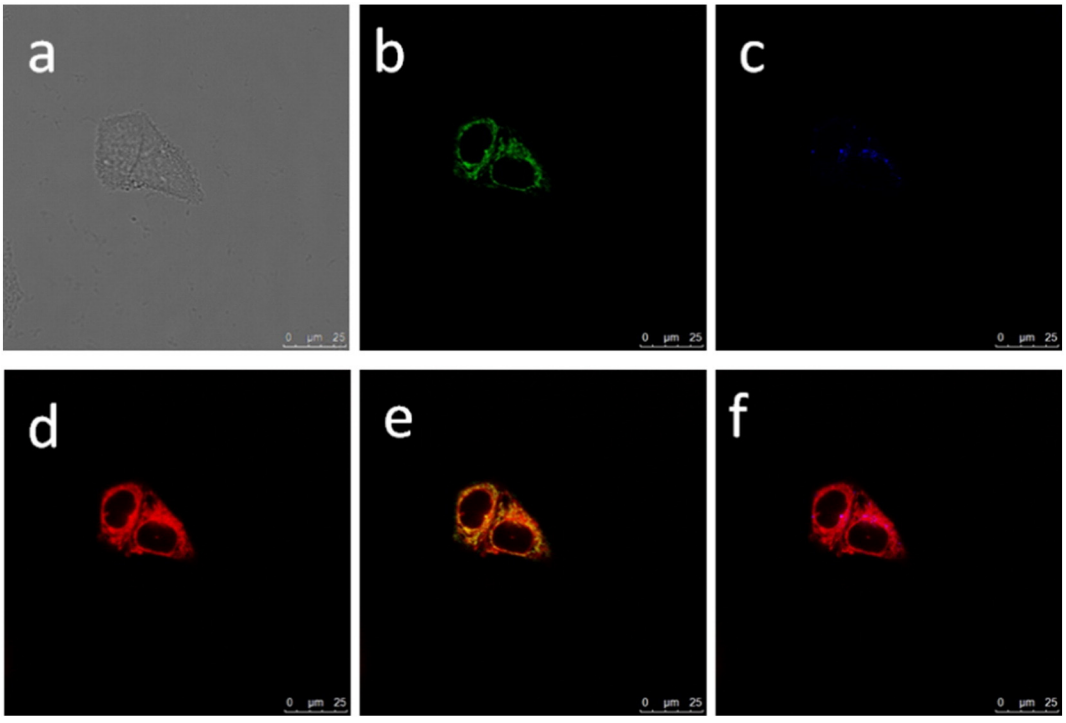

Fig. 5. Visualization of the intracellular fluorescence of HepG2 cells by using filter sets specific for (a) Bright field image, (b) Mito Tracker Green (in green), (c) Lyso Tracker Red (in blue), (d) SiPc **1** (in red), and the corresponding superimposed image of (e) SiPc-Mito Tracker Green and (f) SiPc-Lyso Tracker Red. Scale bar: 25 μm. (For interpretation of the references to color in this figure legend, the reader is referred to the web version of this article.)

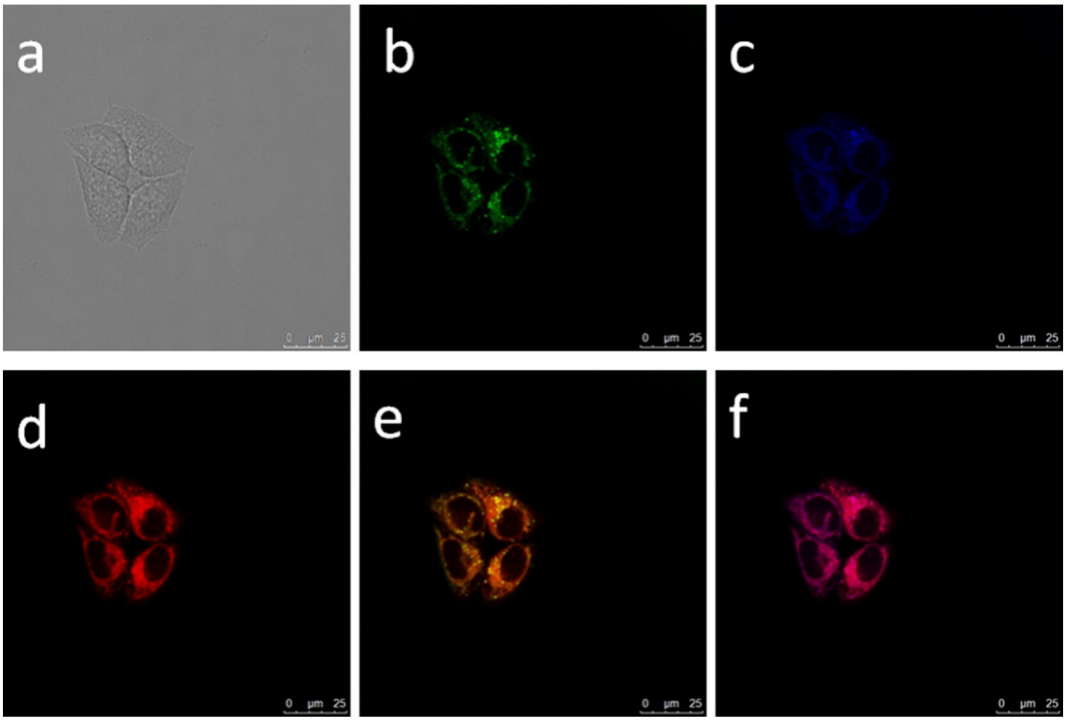

Fig. 6. Visualization of the intracellular fluorescence of HepG2 cells by using filter sets specific for (a) Bright field image, (b) Mito Tracker Green (in green), (c) Lyso Tracker Red (in blue), (d) SiPc **2** (in red), and the corresponding superimposed image of (e) SiPc-Mito Tracker Green and (f) SiPc-Lyso Tracker Red. Scale bar: 25 μm. (For interpretation of the references to color in this figure legend, the reader is referred to the web version of this article.)

cells and BGC823 human gastric cancer cells. Fig. 3 shows the cytotoxicity of **1** and **2** toward both cell lines in the presence or absence of light. It can be seen that these compounds are essentially non-cytotoxic in the dark, but exhibit high photocytotoxicity toward both cell lines with the IC_{50} values ranging from 9 nM to 33 nM (Table 2). For the two cell lines, HepG2 cells are more susceptive to the photosensitizers. By comparison, compound **1** substituted with monochloro-adenosine derivative is slightly more potent than the analog with dichloro-modified nucleoside derivative (compound **2**). Moreover, the photocytotoxicity of compound **1** against HepG2 cells is comparable with the most potent uridine-substituted analog **11** (IC_{50} = 6 nM) among these nucleoside-substituted SiPcs [18]. On the other hand, both compounds (**1** and **2**) show significantly higher photocytotoxicity than a positive control, chlorin e6 (Ce6), a well-known anticancer photosensitizer [4], with an IC_{50} value of 752 nM against HepG2 cells in the same experimental condition (Fig. S2).

3.3.2. Cellular Uptake

The cellular uptake of these SiPcs **1**–**2** and Ce6 by HepG2 cells was also examined by confocal laser scanning microscopy (CLSM) analysis. Fig. 4 shows the bright fields, fluorescence images and the intracellular fluorescence intensities. It can be seen that compound **1** exhibits a slightly stronger fluorescence intensity in the cells than that of **2**. The trend is consistent with the results of photocytotoxicity. On the other hand, the intracellular fluorescence of both SiPcs **1** and **2** is greatly stronger than that of Ce6 (about 39–62 folds in intensity) in the same experimental conditions. Taking the different fluorescence generation efficiency of the SiPcs **1**–**2** and Ce6 into account, the fluorescence spectra of **1** and Ce6 were further measured in DMF (Fig. S3). The fluorescence intensity of compound **1** is about 3-fold higher than that of Ce6. Thus, it can be concluded that the significantly stronger intracellular fluorescence intensity of the SiPcs in contrast to Ce6 is mainly due to the higher cellular uptake. To confirm this viewpoint, we further employed an extraction method to quantify the cellular uptake. After incubation with these photosensitizers for 2 h, DMF was used to lyze the cells and extract the dyes. The dye concentrations inside the cells were quantified by measuring their Q band absorbance. As shown in Fig. 4c, the uptakes of these compounds follow the trend: **1** > **2** > Ce6. This result is in accord with intracellular fluorescence intensity analysis previously, which should be one of the reasons for their large difference in photocytotoxicities.

3.3.3. Subcellular Localization

Since mitochondrion is an important target of the initiation of apoptosis [37–39], we are interested in whether the photosensitizer has an affinity to the mitochondria. Therefore, the subcellular localization of SiPcs **1** and **2** in HepG2 and BGC823 cells were investigated by CLSM. After incubation with the photosensitizers, the cells were stained with MitoTracker Green, which is a specific fluorescence probes for mitochondria. As shown in Fig. 5, the fluorescence of compound **1** in HepG2 cells is essentially overlapped with that of MitoTracker Green and partially superimposed with Lyso Tracker Red, demonstrating that **1** accumulates mainly into mitochondria of HepG2 cells. But the fluorescence of compound **2** compared to MitoTracker Green and Lyso Tracker Red both just partially superimposed, indicating compound **2** is partly localized in mitochondria and lysosomes of HepG2 cells (Fig. 6). For BGC823 cells, similar results could be observed according to the fluorescence images of **1**, **2**, and MitoTracker Green (Fig. S4 in ESI†).

3.3.4. Apoptosis

The mode of cell death induced by PDT of compounds **1** and **2** was also investigated by using a cell apoptosis/death staining kit, annexin V-fluorescein isothiocyanate (FITC) and propidium iodide (PI), which are the fluorescence probes to distinguish viable cells from dead ones of different stages. The dual fluorescence of annexin V-FITC and PI in HepG2 cells was examined by fluorescence confocal microscopy at 6 h and 24 h after PDT treatment, respectively. As shown in Fig. 7a, after PDT treatment with compound **1** for 6 h, the fluorescence of annexin V-FITC could be observed in more than half of the cells, while there was nearly no PI signal detectable. However, after 24 h, the fluorescence of both annexin V-FITC and PI could be obviously observed in most of HepG2 cells. These observations indicate that there were viable and

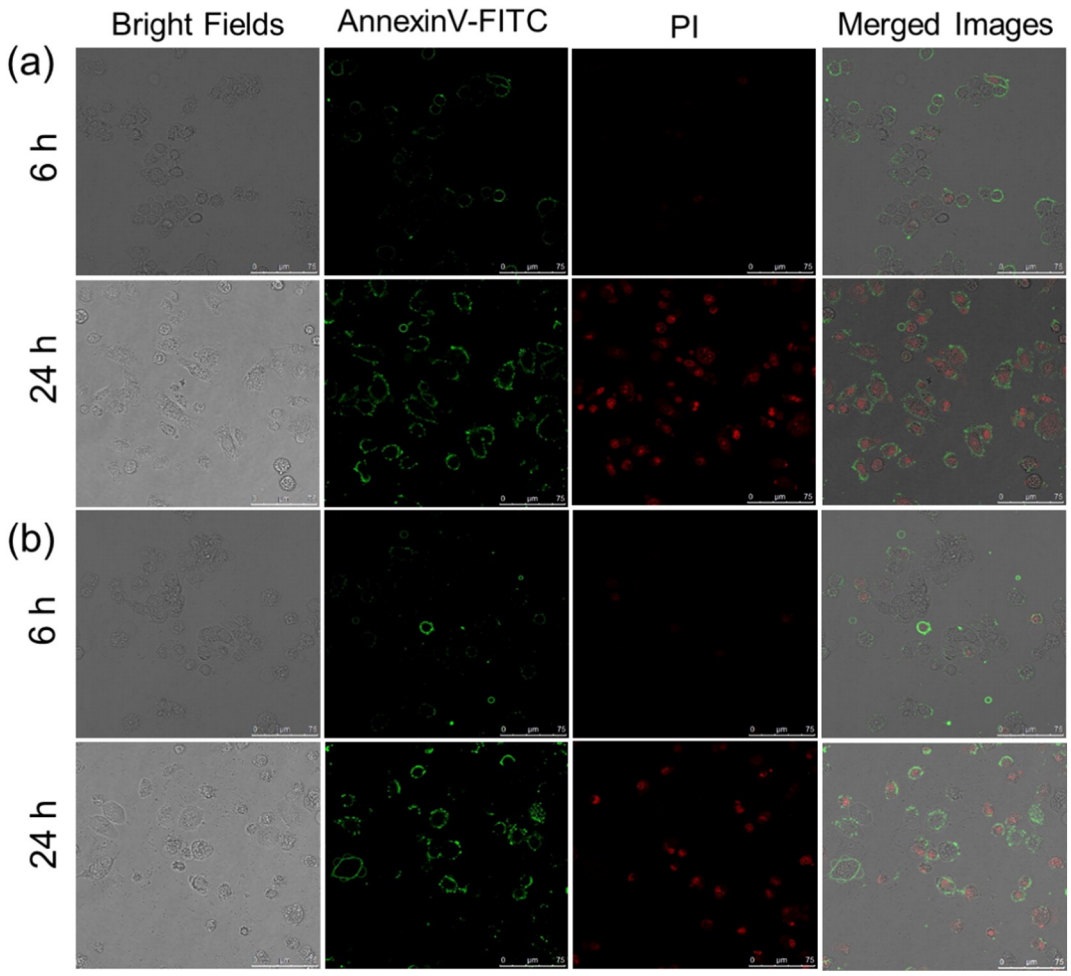

Fig. 7. The intracellular fluorescence images of Annexin V-FITC (in green) and PI (in red) in HepG2 cells after PDT treatment with (a) **1** or (b) **2** (both at 20 nM) for 6 h and 24 h. The bright field and merged images are given in column 1 and 4, respectively. Scale bar: 75 μm. (For interpretation of the references to color in this figure legend, the reader is referred to the web version of this article.)

early apoptotic cells after PDT treatment with **1** for 6 h, and the cells were almost at necrotic or late apoptotic stage after 24 h. For the cells PDT-treated with compound **2**, similar result could be seen after 6 h, but after 24 h, apart from the necrotic or late-stage apoptotic cells, there were still a few early apoptotic ones (Fig. 7b). Therefore, it can be concluded that HepG2 cells underwent an apoptotic process when PDT-treated with both **1** and **2**.

4. Conclusions

A series of new silicon(IV) phthalocyanines (SiPcs) di-substituted axially with different nucleoside moieties have been synthesized and evaluated for their spectroscopic properties, singlet oxygen quantum yields (Φ_Δ) and *in vitro* photodynamic activities. The adenosine-substituted SiPc shows a lower photosensitizing efficiency (Φ_Δ = 0.35) than the uridine- and cytidine-substituted analogs (Φ_Δ = 0.42–0.44), while the guanosine-substituted SiPc exhibits a weakest singlet oxygen generation efficiency with a Φ_Δ value down to 0.03. Moreover, when replacing axial adenosines with monochloro-modified adenosines, the corresponding SiPc **1** gives higher singlet oxygen generation efficiency due to the electron-withdrawing effects of chlorine atom, which decrease the PET effects of amine groups. In view of the high singlet oxygen quantum yields (Φ_Δ = 0.42–0.44), *in vitro* photodynamic activities of **1** and **2** were further evaluated. They are both highly cytotoxic toward HepG2 and BGC823 cells upon illumination with IC_{50} values ranging from 9 nM to 33 nM. Moreover, the photocytotoxities of both compounds **1** and **2** are significantly higher than that of the well-known photosensitizer Ce6 (IC_{50} = 752 nM against HepG2 cells). For both cell lines, compound **1** can essentially bind to mitochondria, while compound **2** is just partially localized in mitochondria. The two compounds can induce cell death of HepG2 cells likely through apoptosis.

Acknowledgments

This work was supported by the Natural Science Foundation of China (Grant Nos. 21172037, 21301031, 21473033), the Public Science and Technology Research Funds Projects of Ocean, China (Grant No. 201305015-2), and Scientific Research Fund of the National Board of Health and Family Planning (the Joint Research Project of Health and Education of Fujian), China (Grant No. WKJ-FJ-32).

Appendix A. Supplementary data

Supplementary data to this article can be found online at http://dx.doi.org/10.1016/j.jphotobiol.2016.03.055.

References

[1] C. Robertson, D.H. Evans, H. Abrahamse, Photodynamic therapy (PDT): A short review on cellular mechanisms and cancer research applications for PDT, J. Photochem. Photobiol. B Biol. 96 (2009) 1–8.
[2] D.E. Dolmans, D. Fukumura, R.K. Jain, Photodynamic therapy for cancer, Nat. Rev. Cancer 3 (2003) 380–387.

[3] S.B. Brown, E.A. Brown, I. Walker, The present and future role of photodynamic therapy in cancer treatment, Lancet Oncol. 5 (2004) 497–508.
[4] M.R. Detty, S.L. Gibson, S.J. Wagner, Current clinical and preclinical photosensitizers for use in photodynamic therapy, J. Med. Chem. 47 (2004) 3897–3915.
[5] D. Samaroo, E. Perez, A. Aggarwal, A. Wills, N. O'Connor, Strategies for delivering porphyrinoid-based photosensitizers in therapeutic applications, Ther. Deliv. 5 (2014) 859–872.
[6] F. Schmitt, L. Juillerat-Jeanneret, Drug targeting strategies for photodynamic therapy, Anti Cancer Agents Med. Chem. 12 (2012) 500–525.
[7] N. Shirasu, S.O. Nam, M. Kuroki, Tumor-targeted photodynamic therapy, Anticancer Res. 33 (2013) 2823–2831.
[8] A.M. Bugaj, Targeted photodynamic therapy—a promising strategy of tumor treatment, Photochem. Photobiol. Sci. 10 (2011) 1097–1109.
[9] J.-P. Taquet, C. Frochot, V. Manneville, M. Barberi-Heyob, Phthalocyanines covalently bound to biomolecules for a targeted photodynamic therapy, Curr. Med. Chem. 14 (2007) 1673–1687.
[10] W.M. Sharman, J.E. van Lier, C.M. Allen, Targeted photodynamic therapy via receptor mediated delivery systems, Adv. Drug Deliv. Rev. 56 (2004) 53–76.
[11] G.A.M.S. van Dongen, G.W.M. Visser, M.B. Vrouenraets, Photosensitizer-antibody conjugates for detection and therapy of cancer, Adv. Drug Deliv. Rev. 56 (2004) 31–52.
[12] R. Schneider, F. Schmitt, C. Frochot, Y. Fort, N. Lourette, F. Guillemin, J.-F. Mullerd, M. Barberi-Heyob, Design, synthesis, and biological evaluation of folic acid targeted tetraphenylporphyrin as novel photosensitizers for selective photodynamic therapy, Bioorg. Med. Chem. 13 (2005) 2799–2808.
[13] M.R. Ke, S.L. Yeung, W.P. Fong, D.K. Ng, P.C. Lo, A phthalocyanine–peptide conjugate with high in vitro photodynamic activity and enhanced in vivo tumor retention property, Chem. Eur. J. 18 (2012) 4225–4233.
[14] A.C. Tedesco, J.C.G. Rotta, C.N. Lunardi, Synthesis, photophysical and photochemical aspects of phthalocyanines for photodynamic therapy, Curr. Org. Chem. 7 (2003) 187–196.
[15] C.M. Allen, W.M. Sharman, J.E. van Lier, Current status of phthalocyanines in the photodynamic therapy of cancer, J. Porphyrins Phthalocyanines 5 (2001) 161–169.
[16] E.A. Lukyanets, Phthalocyanines as photosensitizers in the photodynamic therapy of cancer, J. Porphyrins Phthalocyanines 3 (1999) 424–432.
[17] Y.-W. Zheng, S.-F. Chen, B.-Y. Zheng, M.-R. Ke, J.-D. Huang, A silicon(IV) phthalocyanine-folate conjugate as an efficient photosensitizer, Chem. Lett. 43 (2014) 1701–1703.
[18] X.M. Shen, B.Y. Zheng, X.R. Huang, L. Wang, J.D. Huang, The first silicon(IV) phthalocyanine-nucleoside conjugates with high photodynamic activity, Dalton Trans. 42 (2013) 10398–10403.
[19] M. Mitsunaga, M. Ogawa, N. Kosaka, L.T. Rosenblum, P.L. Choyke, H. Kobayashi, Cancer cell-selective in vivo near infrared photoimmunotherapy targeting specific membrane molecules, Nat. Med. 17 (2011) 1685–1691.
[20] P.-C. Lo, C.M. Chan, J.-Y. Liu, W.-P. Fong, D.K. Ng, Highly photocytotoxic glucosylated silicon (IV) phthalocyanines. Effects of peripheral chloro substitution on the photophysical and photodynamic properties, J. Med. Chem. 50 (2007) 2100–2107.
[21] T. Nyokong, Effects of substituents on the photochemical and photophysical properties of main group metal phthalocyanines, Coord. Chem. Rev. 251 (2007) 1707–1722.
[22] G. Zheng, J. Chen, H. Li, J.D. Glickson, Rerouting lipoprotein nanoparticles to selected alternate receptors for the targeted delivery of cancer diagnostic and therapeutic agents, Proc. Natl. Acad. Sci. U. S. A. 102 (2005) 17757–17762.
[23] L. Alexandrova, 4′-C-nucleoside derivatives: synthesis and antiviral properties, Rus. J. Bioorg. Chem. 37 (2011) 651–671.
[24] N. Tzioumaki, E. Tsoukala, S. Manta, G. Agelis, J. Balzarini, D. Komiotis, Synthesis, antiviral and cytostatic evaluation of unsaturated exomethylene and keto D-lyxopyranonucleoside analogues, Arch. Pharm. Chem. Life Sci. 342 (2009) 353–360.
[25] A. Matsuda, T. Sasaki, Antitumor activity of sugar-modified cytosine nucleosides, Cancer Sci. 95 (2004) 105–111.
[26] P. Patel, H.H. Patel, E. Borland, S.M. Gorun, D. Sabatino, Chemically robust fluoroalkyl phthalocyanine–oligonucleotide bioconjugates and their GRP78 oncogene photocleavage activity, Chem. Commun. 50 (2014) 6309–6311.
[27] T. Torres, A. Gouloumis, D. Sanchez-Garcia, J. Jayawickramarajah, W. Seitz, D.M. Guldi, J.L. Sessler, Photophysical characterization of a cytidine–guanosine tethered phthalocyanine–fullerene dyad, Chem. Commun. 3 (2007) 292–294.
[28] R.O. Ogbodu, E.K. Amuhaya, P. Mashazi, T. Nyokong, Photophysical properties of zinc phthalocyanine–uridine single walled carbon nanotube-conjugates, Spectrochim. Acta A Mol. Biomol. Spectrosc. 149 (2015) 231–239.
[29] X.-Y. Li, D.K. Ng, Synthesis and spectroscopic properties of the first phthalocyanine–nucleobase conjugates, Tetrahedron Lett. 42 (2001) 305–309.
[30] M.R. Reddy, N. Shibata, Y. Kondo, S. Nakamura, T. Toru, Design, synthesis, and spectroscopic investigation of zinc dodecakis (trifluoroethoxy) phthalocyanines conjugated with deoxyribonucleosides, Angew. Chem. Int. Ed. 45 (2006) 8163–8166.
[31] J.L. Sessler, J. Jayawickramarajah, A. Gouloumis, G. Dan Pantos, T. Torres, D.M. Guldi, Guanosine and fullerene derived de-aggregation of a new phthalocyanine-linked cytidine derivative, Tetrahedron 62 (2006) 2123–2131.
[32] X.-M. Shen, X.-J. Jiang, C.-C. Huang, H.-H. Zhang, J.-D. Huang, Highly photostable silicon(IV) phthalocyanines containing adamantane moieties: synthesis, structure, and properties, Tetrahedron 66 (2010) 9041–9048.
[33] I. Scalise, E.N. Durantini, Synthesis, properties, and photodynamic inactivation of *Escherichia coli* using a cationic and a noncharged Zn (II) pyridyloxyphthalocyanine derivatives, Bioorg. Med. Chem. 13 (2005) 3037–3045.
[34] M.D. Maree, N. Kuznetsova, T. Nyokong, Silicon octaphenoxyphthalocyanines: photostability and singlet oxygen quantum yields, J. Photochem. Photobiol. A Chem. 140 (2001) 117–125.
[35] X.J. Jiang, P.C. Lo, S.L. Yeung, W.P. Fong, D.K.P. Ng, Phthalocyanine-polyamine conjugates as highly efficient photosensitizers for photodynamic therapy, J. Med. Chem. 54 (2011) 320–330.
[36] X.F. Zhang, X. Li, L. Niu, L. Sun, L. Liu, Charge transfer Photophysics of tetra(α-amino) zinc phthalocyanine, J. Fluoresc. 19 (2009) 947–954.
[37] J. Morgan, A.R. Oseroff, Mitochondria-based photodynamic anti-cancer therapy, Adv. Drug Deliv. Rev. 49 (2001) 71–86.
[38] P. Mroz, A. Yaroslavsky, G.B. Kharkwal, M.R. Hamblin, Cell death pathways in photodynamic therapy of cancer, Cancer 3 (2011) 2516–2539.
[39] Y. Ge, X. Weng, T. Tian, F. Ding, R. Huang, L. Yuan, J. Wu, T. Wang, P. Guo, X. Zhou, A mitochondria-targeted zinc(II) phthalocyanine for photodynamic therapy, RSC Adv. 3 (2013) 12839–12846.